Silicon (2023) 15:813–827
https://doi.org/10.1007/s12633-022-02046-2

ORIGINAL PAPER

Influence of Process Parameters on Microstructure and Mechanical Properties ofAS21-SiC Composites through Two-Step Stir-Casting

D. Rognatha Rao[1] · **C. Srinivas**[2]

Received: 14 April 2022 / Accepted: 27 July 2022 / Published online: 10 August 2022

Abstract

This work aims to focus on fine precipitation of Mg-Si compound in AS21 alloy system by the dispersion of SiC reinforcement through stir-casting in two steps. Dual step stir-casting at a melt temperature of 680 º C, 700 º C, and 720 º C with varied stirring rates (S) manufactured the AS21 alloy composite having 2, 4 and 6 wt.% of SiC. The Taguchi L_9 experiments were implemented with three processing factors (wt.% of reinforcement, melt temperature and stirring speed) at three levels in order to acquire optimum conditions. Metallographic examinations depict the formation fine grain structure and precipitation of fine Mg-Si compound with the SiC reinforcement. The ANOVA analysis identified the SiC reinforcement as the most effective parameter influencing the mechanical properties of AS21 alloy composites. The tensile strength of 199.35 MPa was attained at the optimum two-step stir casting conditions: i.e. melt temperature of 720 º C, stirring speed of 600 rpm by adding 6 wt.% of SiC in AS21 alloy. The influence of SiC variation on Mg_2Si compound by duel step stir casting were discussed in detail.

Keywords AS21 alloy · SiC reinforcement · Mg_2Si phase · Grain refinement · Melt temperature · Mechanical properties

1 Introduction

Magnesium (Mg) alloys are contemplating the most capable materials in aerospace and automotive industries. Furthermore, magnesium metal matrix composites also expose good cast-ability, machinability, thermal stability and damping properties [1]. Synthesis and fabrication of Mg metal matrix composite is the great challenge for researchers and scientists for the reason that high affinity of magnesium towards oxygen. Casting route gained more attention to produce Mg alloy composites for the structural application of magnesium [2]. Vacuum assisted stir-casting of Mg alloy and its composites as one of the sustainable process due to its near net shape components in a cost effective manner [3].

In general, SiC reinforcement has become great interest and is the most commonly used reinforcement for Mg and Al alloys because of its excellent compatibility, high damping characteristics, increase in dimensional stability and low cost [4–6]. Researchers found that SiC reinforcing micro-particles by stir-casting can be effectively enhanced the mechanical and wear properties of the composites [7–9]. Micro-scaled reinforcements rather than Nano-reinforcements are easily dispersed and very economical in industries for attaining attractive properties of Mg alloy composites [10, 11].

Stirring technique shows a noticeable impact on the reinforcement distribution in the base matrix at liquid state and also manufactures the near net shaped components [12, 13]. But some of the structural defects such as particle cluster, porosity and surface oxidation arise during fabrication by conventional casting route [14]. Recently, two-step stir-casting was adopted to overcome these pitfalls during fabrication of metal matrix composites [15]. Qiyao et al. [16] characterized the microstructure and mechanical properties of Al composites by two-step stir-casting. The authors found more uniform particle distribution and fewer interfacial compounds was formed by this process. Pagidiet al. [17] fabricated the Al-hBN nano-composites by two-step stir-casting. The microstructure revealed major compounds of Al and hBN nano-particles with no impurities.

✉ D. Rognatha Rao
drognath@gmail.com

1 Department of Mechanical Engineering, Acharya Nagarjuna University, Guntur, Andhra Pradesh 522510, India

2 Department of Mechanical Engineering, R.V.R.&.J.C college of Engineering, Chowdavaram, Andhra Pradesh 522019, India

Among the available Mg alloys, Mg-Si alloy was potential material for engineering applications. AS21 is an Mg-Al-Si alloy which has excellent cast-ability and superior mechanical properties.The excess Si reacts with Mg and forms as an intermetallic phase of Mg_2Si which improves mechanical and creep properties [18]. These alloys exhibit superior elevated temperature properties and also to be utilized as structural parts in automotive and aerospace applications [19]. The intermetallic compound of Mg-Si phase obtained via conventional casting has a coarse size leading to highly brittle and deterioration of material properties [20]. Therefore, the finer size of Mg-Si precipitate in AS21 alloy is desired for better improvement of mechanical properties.

In the view from above literature, a metal matrix composite by two-step stir-casting was studied in a limited way. To the best of the author's knowledge, no reports are available on the development of AS21 Mg alloy composites. In the present investigation, the fabrication of AS21 alloy and its composites with SiC reinforcement was done through a two-step stir-casting for the first time. The operating parameters such as melt temperature, stirring speed and SiC reinforcement were chosen at three different levels and optimized by a Taguchi L9 approach to attain superior mechanical properties.

Fig. 1 Specimens cast of AS21-SiC composites

2 Fabrication Procedure

Commercially available magnesium AS21 Mg alloy ingot (Venuka Engineering Pvt. Ltd., India, 99.7%, 100 µm) with a nominal composition of Mg-2.11Al-1.03Si-0.23Mn was chosen as base matrix. The reinforcement percentage of SiC (Alfa Aesar, India, 99.95%, 10 µm) was varied from 2 wt.% to 6 wt.% in steps of 2% to prepare AS21 composite. Premeasured quantity of Mg alloy AS21 was melted in an electrical resistance furnace at three different temperatures (680 °C, 700 °C and 720 °C) under an inert atmosphere. To obtain Mg AS21 composite, a known quantity of SiC particles was carefully weighed and added to magnesium alloy melt. The SiC particles are primarily pre-heated in a muffle furnace to eliminate moisture from particulates and increase wett-ability in a matrix material. The preheated reinforcement particles were mixed with AS21 melt through stirrer for 15 min. Stirring was done at three different speeds of 400 rpm, 500 rpm and 600 rpm respectively. The melt temperature was brought down to 650 °C, and then heated rapidly to 750 °C. Finally the composite melt was poured into a preheated gray cast iron cylindrical mold and then the mold is allowed to cool for a few minutes. Homogenization of Mg alloy and composites was done for 12 hours to get rid of residual stresses. A cover flux 1 Wt.% of matrix was used to remove the dissolved gases and to prevent oxidation in the molten metal during melting process.

Table 1 Details of AS21-SiC composite fabrication parameters

Parameters	Unit	Level 1	Level 2	Level 3
SiC Reinforcement (SiC)	Wt.%	2	4	6
Melt temperature (Tm)	^{o} C	680	700	720
Stirring speed (S)	rpm	400	500	600

The samples of AS21 composites (Fig. 1) were then machined by ASTM standards for microstructural analysis and mechanical tests. Microstructure analysis was contemplated using a scanning electron microscope (Hitachi S300N, Japan). Density of the Mg composite solid sample was estimated by mass and physical dimensions. Micro-hardness was measured with a dwell period of 10s at a load of 100 g in several regions of the Mg composite surface. Tensile strength was estimated using computerized Instron-8801 UTM with a ram speed of 3 mm/min at room temperature as per ASTM E-8 standard. The parameters for processing AS21-SiCmetal matrix composites were optimized using Taguchi L_9approach. Table 1 illustrates the levels of variation of process parameters in this research work.

3 Results and Discussions

3.1 Microstructure

Figure 2a-d shows the SEM microstructure of AS21 Mg alloy and composites at different levels of process parameters. The microstructures reveal presence of gray particles in different regions of Mg alloy and composites. Many of gray particles settled near grain boundaries surrounded by dark region. The non-uniform dispersion of gray particles and uneven grain boundaries are observed in the microstructure of AS21 Mg alloy. However, the dispersion is uniform with the addition of SiC reinforcement. The AS21 Mg composite fabricated with the operating parameters 2%SiC, 720 °C and 600 rpm (Fig. 2b) shows fine grains with clear grain boundary intersection. The microstructure is more uniform with the increase in volume fraction of SiC reinforcement (Fig. 2c and d).

In order to identify the elemental distribution in the microstructure of AS21 composites an SEM-EDS analysis was performed in different regions. Figure 3a and b shows SEM with EDS spectra at different points of the microstructures. At point '+1' marked in the microstructures shows the elemental distribution of AS21 composition. However, the point marked in '+2' of gray particles shows the elemental distribution of Mg and Si only. This EDS elemental distribution suggests the precipitation of intermetallic compound of Mg_2Si composition. The elemental concentration of Si in gray particles (point '+2') of AS21 and AS21–6%SiC are 33.41% and 30.58%. This observation suggests that the stoichiometric ratio of magnesium and silicon is nearer to Mg_2Si compound [21]. Similar observations were notified

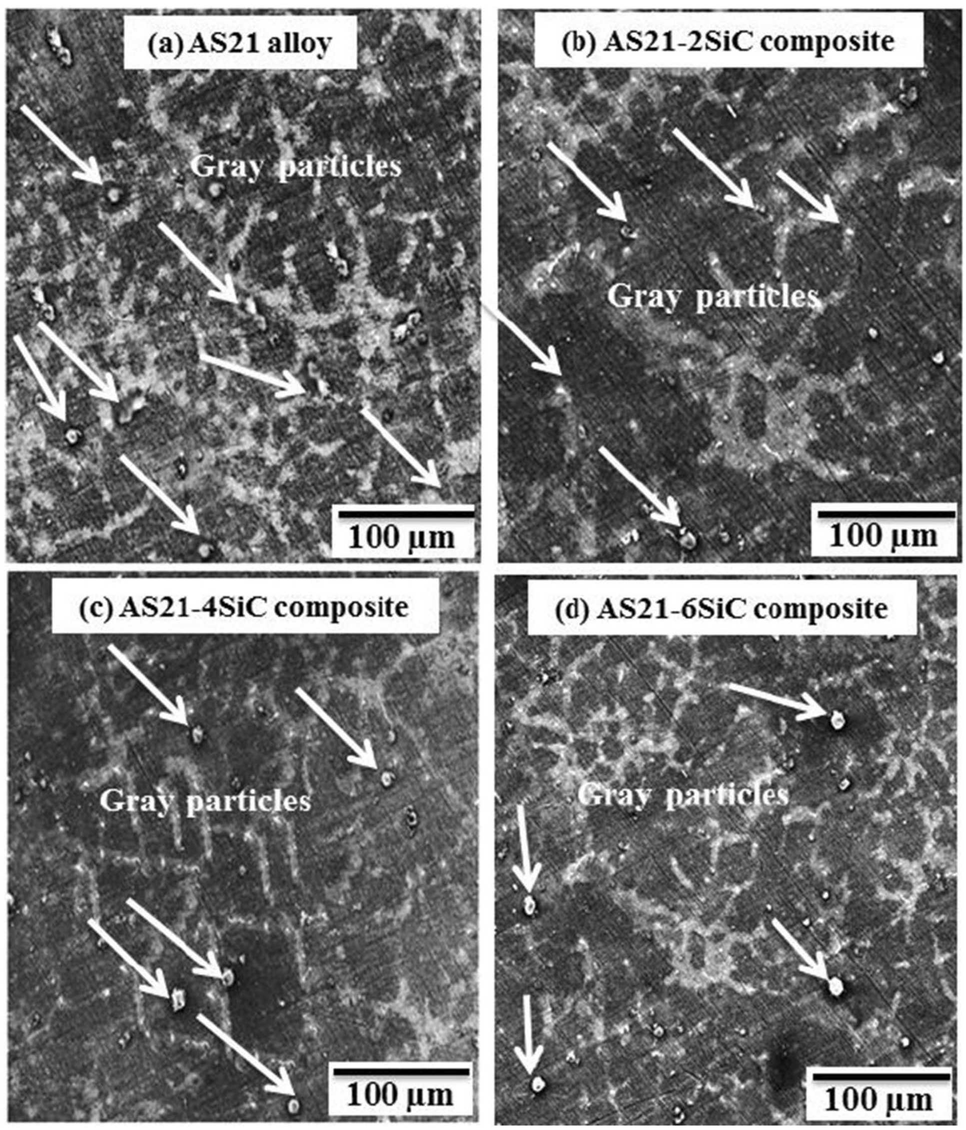

Fig. 2 SEM images of AS21 composite at different process parameters (SiC, Tm and S): (**a**) 0%, 720 °C, 600 rpm; (**b**) 2%, 720 °C, 600 rpm;(**c**) 4%, 720 °C, 600 rpm; (**d**) 6%, 720 °C, 600 rpm

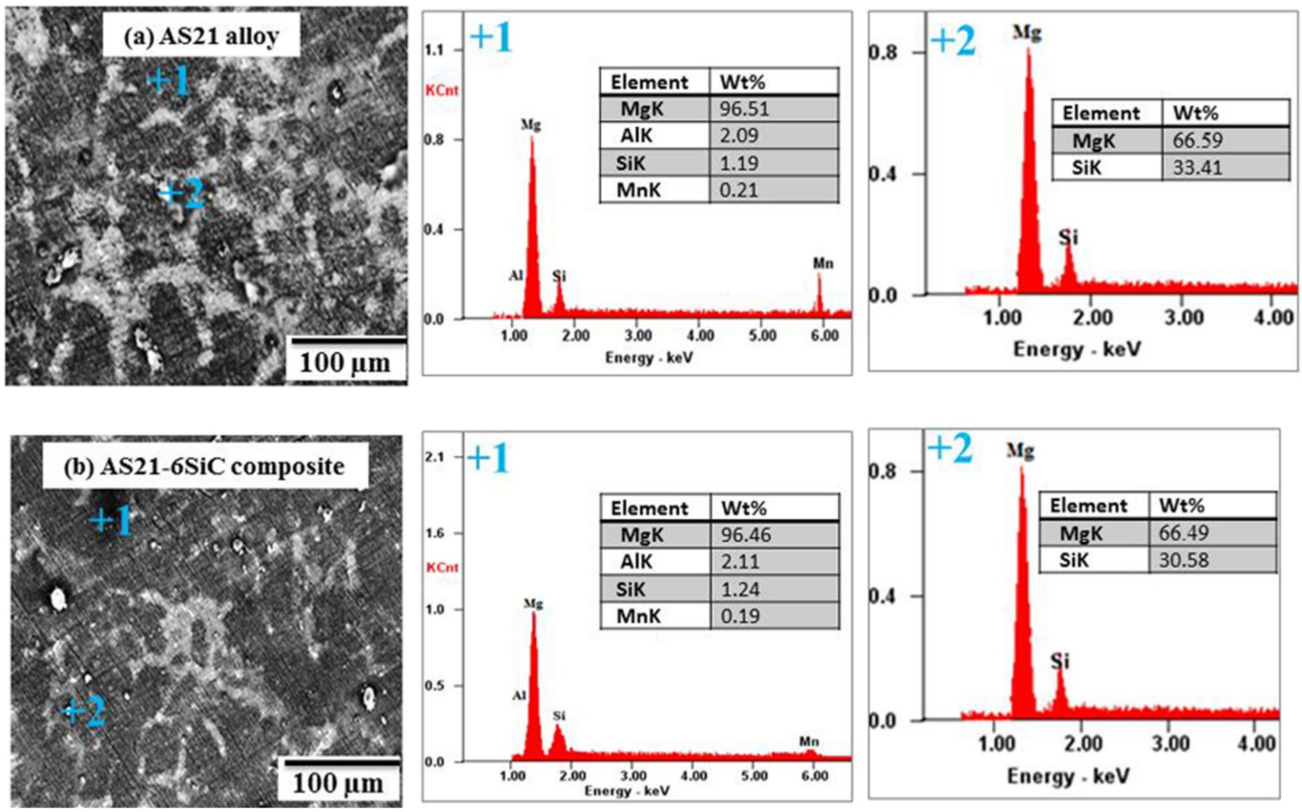

Fig. 3 SEM-EDS of Mg AS21 composites (SiC, Tm and S): (**a**) 0%, 720 °C, 600 rpm; (**b**) 6%, 720 °C, 600 rpm

with the microstructure of AS21–2%SiC and AS21–4%SiC composites.

Figure 4 illustrates the SEM image with EDS spectra of AS21–6%SiC composites. The High intensity of silicon with only carbon is observed in the region. This analysis clearly reveals the existence of SiC reinforcement in AS21 Mg alloy. It is to be noted that irrespective of process parameters, the individual SiC particles were identified in all microstructures of AS21 composites.

Figure 5a-d explains the grain size distribution of AS21 composites at different volume fraction of SiC reinforcement using Image J software. The average grain diameter of AS21 alloy (Fig. 5a) was 61.08 µm. However, the grain diameter is decreased to 54.15 µm with 2% SiC reinforcement (Fig. 5b). The grains were further refined to 45.02 µm with 4% SiC reinforcement (Fig. 5c). The average size of grain after 6% of SiC reinforcement was 40.63 µm (Fig. 5d). The possible reason for refinement of grain is due to pinning effect of uniformly dispersed SiC [22].

3.2 Taguchi Approach

Taguchi optimization [23] is a powerful approach for designing high quality systems formulated on the basis of orthogonal array (OA) experiments. It establishes an integrated approach that is simple and efficient to predict an optimum setting of process control parameters. In the present research, the Taguchi approach is implemented by engaging larger is better S/N (signal to noise) ratio for optimum parameters prediction using MINITAB-21 software. Response characteristics such as hardness and strength were experimented as per L_9 OA. The average of five readings from each experiment was noted as the final values of hardness and tensile strength.

Table 2 exhibits the response characteristics with S/N ratios for three process parameters at three levels executed as per L_9 orthogonal array. Tables 3, 4 and 5 shows the response table of density, hardness and tensile strength for corresponding process parameters. The impact of input factors on the density of AS21 composite was in the order of Melt temperature (^{o} C) > SiC reinforcement (wt.%) > Stirring speed (rpm). However, the impact of input factors on hardness and tensile strength of AS21 composites was in the order of SiC reinforcement (wt.%) > Melt temperature (^{o} C) > Stirring speed (rpm).

To predict the optimum level of operating parameters for density, hardness and tensile strength of AS21 composite, the each level of process parameters has been evaluated by employing main effects plot analysis. Figure 6a-c shows the main effect plot of process parameters for the output

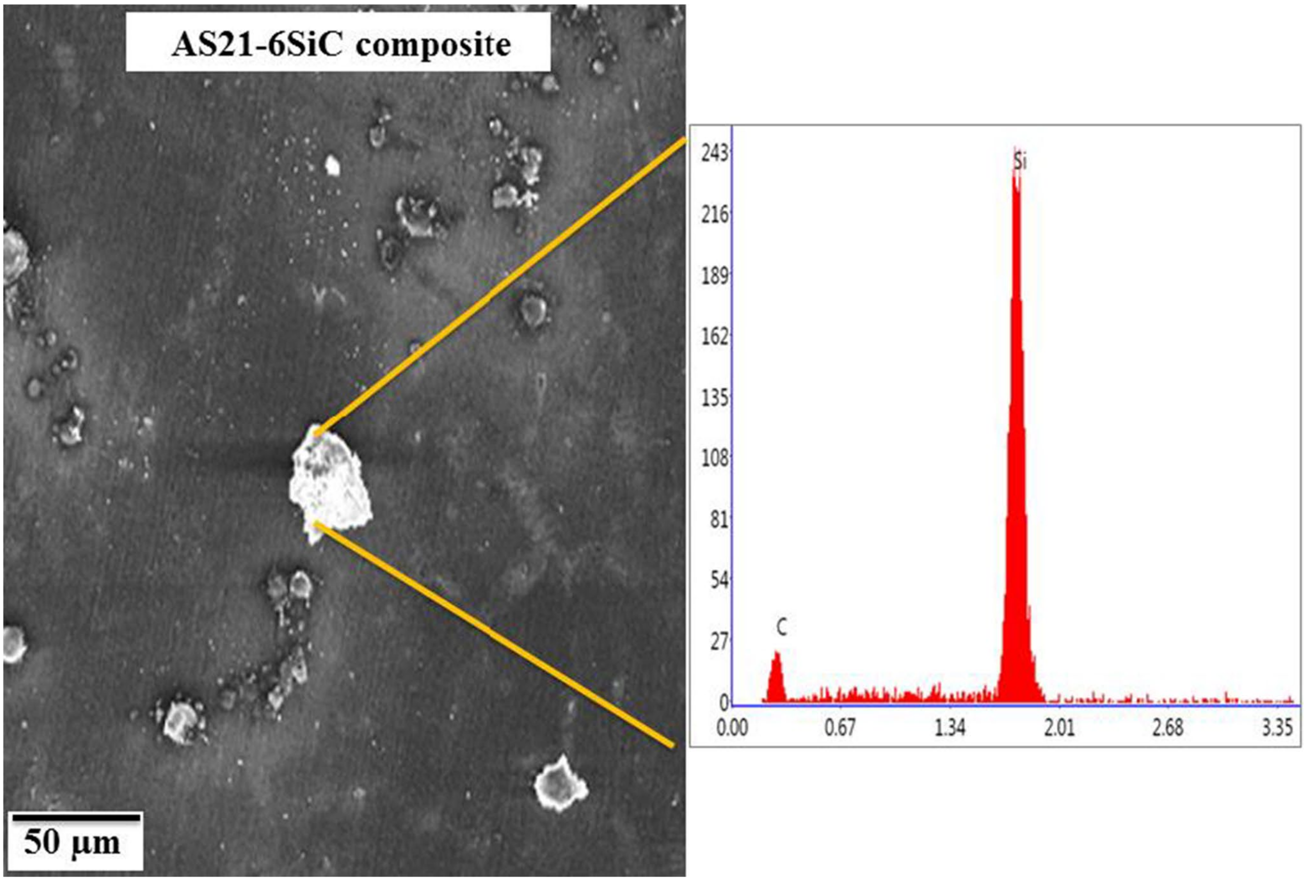

Fig. 4 SEM-EDS of AS21–6%SiC composites

characteristics of density, hardness and tensile strength and the values are listed in Table 6. Figure 7a-c shows the normal probability of density, hardness and tensile strength of the AS21 composite describes more about experimental data consistency. Data is closer to central line indicating that the results are reliable.

3.3 ANOVA Results

ANOVA analysis predicts the significance of each process parameter on multiple quality characteristics [24]. Tables 7, 8 and 9 shows the significance of each input factor on response characteristic of density, hardness and tensile strength. From the ANOVA analysis of density (Table 6), melt temperature is the major contributor with a contribution of 99.59%. SiC reinforcement was identified the most significant parameter on the measurement of hardness with the contribution of 81.70%, followed by melt temperature with a contribution of 16.66%. And also SiC reinforcement is the major contributor with 91.64%, followed by melt temperature of contribution 7.48% on tensile strength measurement. It is to be noted that SiC reinforcement is the major parameter that show significant contribution on mechanical properties of AS21Mg composites. The analysis also shows that R-Sq value is above 90% indicating the results are just adequate.

3.4 Hardness Variation

Figure 8 shows hardness variation of the Mg AS21-SiC composites under different process parameters. The hardness of AS21 alloy fabricated under melting temperature of 720 °C and stirring speed of 600 rpm showed 57.8 HV. However, the hardness increased by 10.67% with the addition of 2% SiC, 18.75% with the addition of 4% SiC and 28.35% with the addition of 6% SiC in the AS21 base matrix. The hardness is significantly improved with the addition of SiC reinforcement. The results of hardness improvement are due to restriction of localized plastic deformation by the dispersion of hard ceramic SiC particles in during the indentation [25].

3.5 Tensile Strength Variation

Figure 9a and b shows the room temperature tensile test specimens and stress-strain curves of AS21 alloy composites. The tensile strength of AS21 mg alloy was 141.69 MPa.

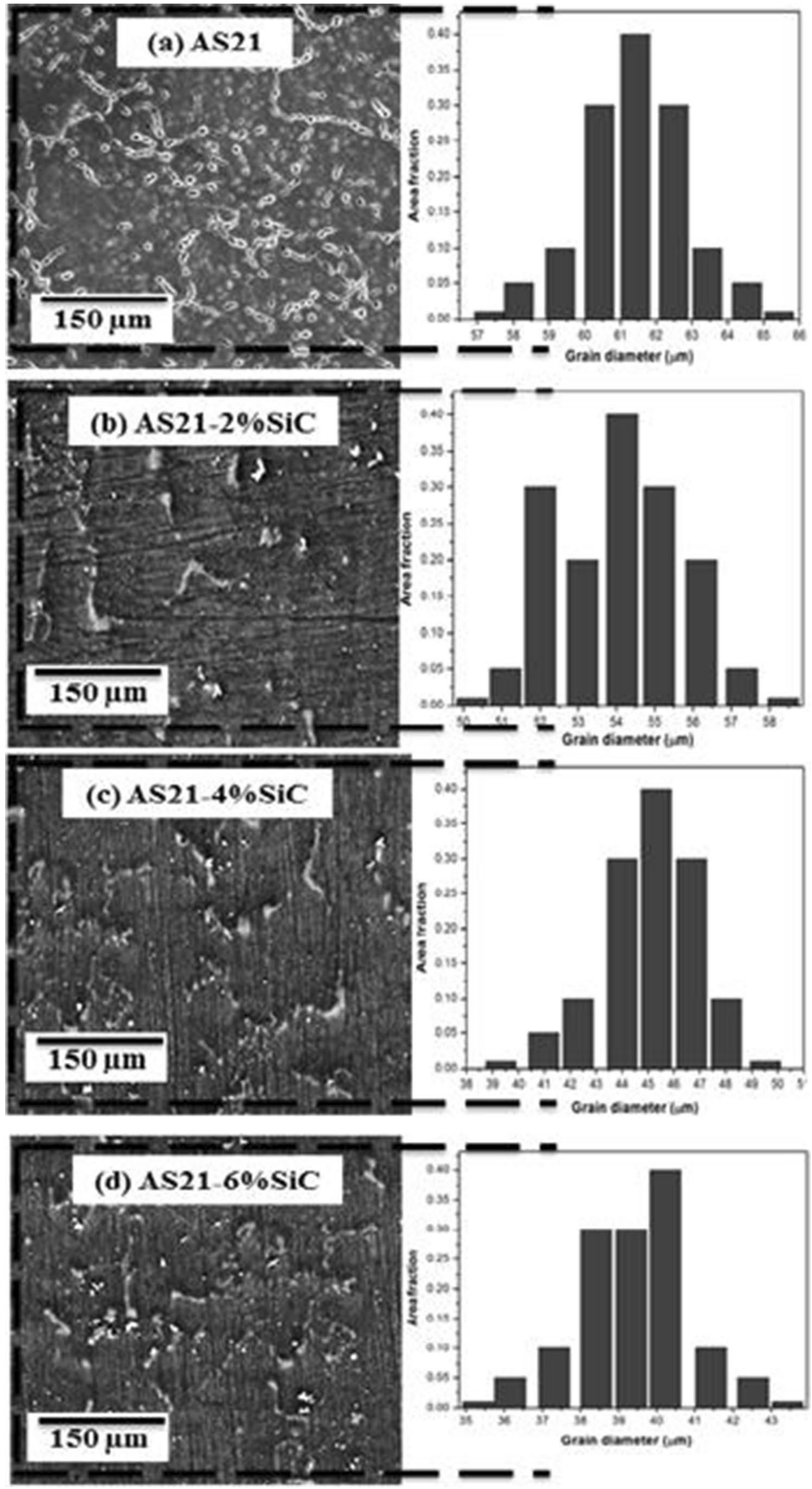

Fig. 5 Grain size distribution of AS21 composites: (**a**) 0% SiC; (**b**) 2% SiC; (**c**) 4% SiC; (**d**) 6% SiC

Table 2 Response characteristics and S/N ratios of AS21-SiC composites

Exp. No	SiC (Wt.%)	Tm (° C)	S (rpm)	Density (%)	S/N Ratio	Hardness (HV)	S/N Ratio	Strength (MPa)	S/N Ratio
1	2	680	400	96.95	39.73	60.18	35.58	149.05	43.46
2	2	700	500	97.86	39.81	62.06	35.85	151.23	43.59
3	2	720	600	98.92	39.90	64.71	36.21	159.31	44.04
4	4	680	500	97.13	39.74	67.08	36.53	161.42	44.15
5	4	700	600	97.53	39.78	71.14	37.04	168.34	44.52
6	4	720	400	98.89	39.90	71.13	37.04	170.51	44.63
7	6	680	600	97.13	39.74	70.23	36.93	186.22	45.40
8	6	700	400	97.86	39.81	74.54	37.44	190.16	45.58
9	6	720	500	98.89	39.90	80.68	38.13	199.35	45.99

Table 3 Response table for density -S/N ratios

Level	SiC (Wt.%)	Tm (° C)	S (rpm)
1	39.82	39.74	39.82
2	39.81	39.80	39.82
3	39.82	39.90	39.81
Delta	0.01	0.16	0.01
Rank	2	1	3

Table 4 Response table for hardness -S/N ratios

Level	SiC (Wt.%)	Tm (° C)	S (rpm)
1	35.89	36.35	36.69
2	36.87	36.78	36.84
3	37.50	37.13	36.73
Delta	1.62	0.78	0.15
Rank	1	2	3

Table 5 Response table for tensile strength -S/N ratios

Level	SiC (Wt.%)	Tm (° C)	S (rpm)
1	43.70	44.34	44.56
2	44.44	44.57	44.58
3	45.66	44.89	44.66
Delta	1.96	0.55	0.10
Rank	1	2	3

The addition of 2% SiC increased the tensile strength to 159.31 MPa. The tensile strength further increased to 170.51 MPa by increasing the volume fraction of SiC from 2% to 4%. On further increase of the SiC volume fraction from 4% to 6%, the tensile strength grows and increased to 199.35 MPa (Fig. 10). From the results, it can be seen that the tensile strength of AS21 alloy increased by 28.92% with the addition of 6% SiC reinforcement. The enhancement in strength of AS21 was attributed to the formation of refined grain structure with 6% SiC reinforcement (Fig. 5d) and strong interfacial bonding between matrix and reinforcement [26].

3.6 Fractography

Figure 11 depicts the fracture SEM images of broken surfaces under tension test of AS21 alloy and its composites. The fracture surface of AS21 alloy (Fig. 11a) indicates more of dimples which indicate the ductile nature of the fracture. The fracture surface of 2 wt.% and 4 wt.% SiC dispersed AS21 alloy (Fig. 11b and c) indicates mixed features of failure patterns which is predominantly dimples and tearing ridges. The refined grain structure by SiC reinforcement is the primary cause for a reduction in the size of dimples in the composite [27]. Moreover, no voids near the hard particles in 6 wt.% of SiC reinforcement (Fig. 11d) indicate strong interface bonding in composite [28]. This may be the cause for improved strength and hardness with higher volume fraction (6%) of SiC reinforcement.

3.7 Discussion on SiC Dispersion by Two-Step Stir Casting

The fabrication of AS21 alloy composites by two-step stir-casting revealed less oxidation of magnesium and no significant micro pores and no perceptible oxide inclusion. The successful consolidation of SiC/AS21 composite shows the right selection of influencing parameters during the duel step process, i.e. wt.% of SiC, melt temperature and stirring speed. The near dense samples at high melt temperature (720 ° C) enables higher diffusion rates, which promote densification process [29]. Dispersion of 2, 4 and 6 wt.% of SiC in the semi solid state with proper control of duel step movement forms homogeneous distribution of SiC in AS21 alloy. Similar results were reported for the density of samples synthesized through two-step by Aravindan [30]. The dual step mixing facilitates the successful amalgamation of SiC reinforcement in AS21 alloy. Moreover, the minimal

Fig. 6 Main effect plot of AS21 composites: (**a**) Density; (**b**) Hardness; (**c**) Tensile strength

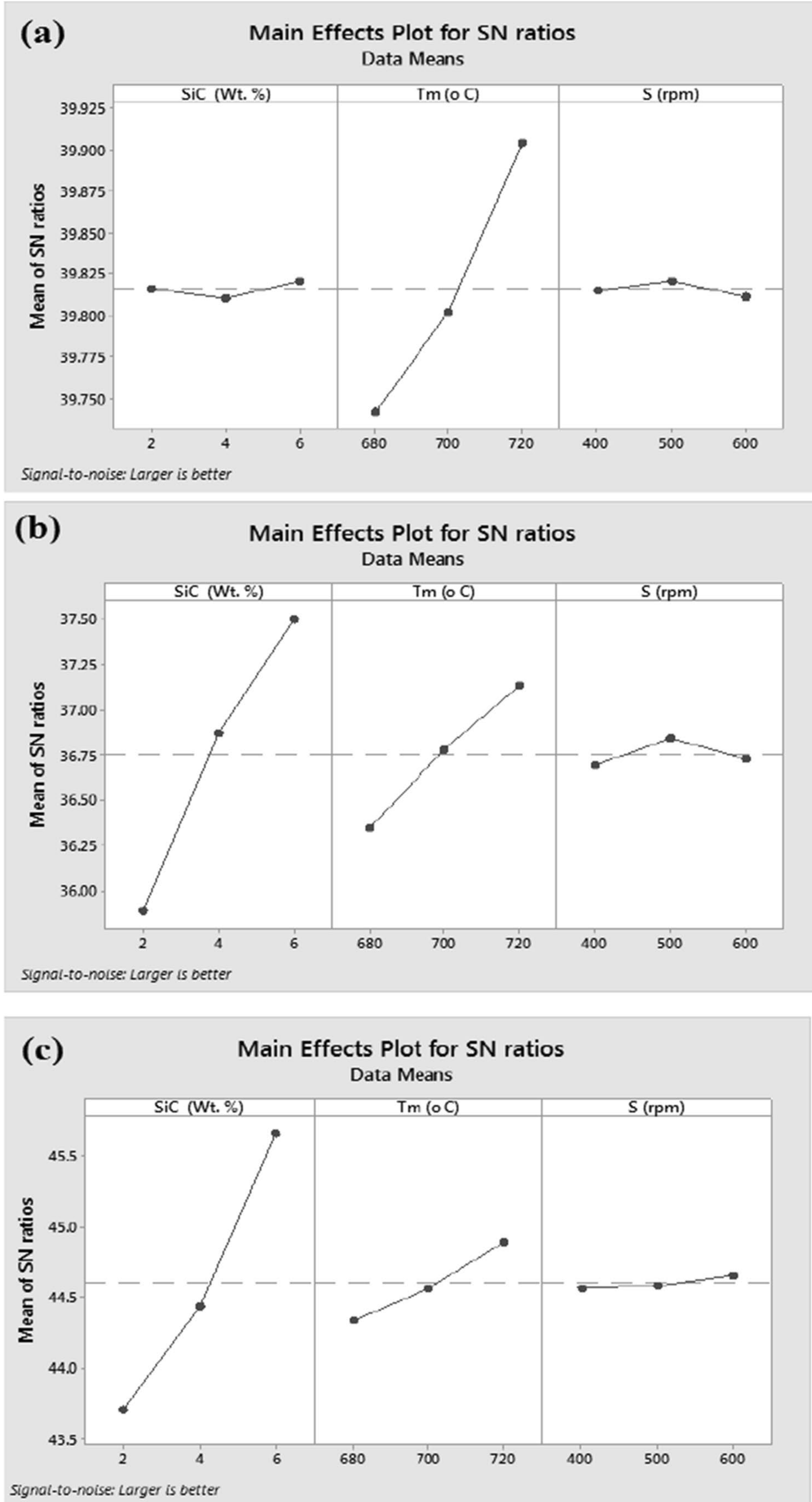

Table 6 Optimum process parameters of AS21-SiC composites

Response characteristics	Optimum level of parameters		
	SiC Reinforcement (Wt.%)	Melt temperature (Tm)	Stirring speed (S)
Density (%)	2	720	600
Hardness (HV)	6	720	500
Tensile strength (Mpa)	6	720	600

wastage from the slurry by two-step mixing confirms the good wettability between AS21 alloy and SiC particles [31]. When increasing the melt temperature from 680 °C to 720 °C, significant improvement in density of AS21 composite was observed.

The microstructure of AS21 alloy and its composites were studied as a function of influencing parameters. The formation of intermetallic compound Mg_2Si is possible due to electro-negativity difference in silicon and magnesium [32]. The precipitation of Mg_2Si phase was dominant and dense

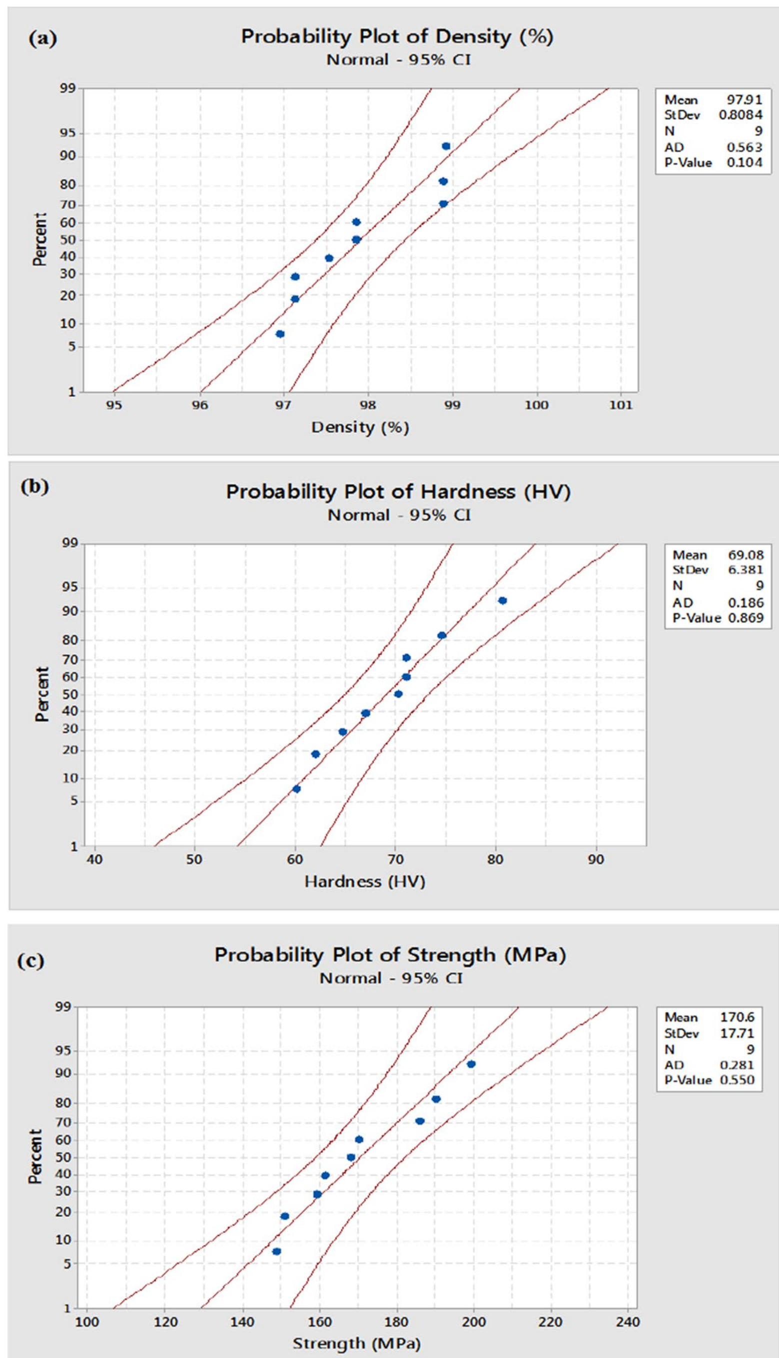

Fig. 7 Normal probability plot of AS21 composite: (**a**) Density; (**b**) Hardness; (**c**) Tensile strength

Table 7 ANOVA analysis for density

Source	DF	Seq. SS	Contribution	Adj. SS	Adj. MS	F-Value	P Value
SiC (Wt.%)	2	0.0187	0.15%	0.0187	0.00935	0.59	0.628
Tm (° C)	2	12.7506	99.59%	12.7506	6.37531	402.9	0.002
S (rpm)	2	0.0025	0.02%	0.0025	0.00126	0.08	0.926
Error	2	0.0316	0.25%	0.0316	0.01582		
Total	8	12.8035	100.00%				
S = 0.125791;		R-sq = 99.75%;		R-sq (adj) = 99.01%;			

Table 8 ANOVA analysis for hardness

Source	DF	Seq. SS	Contribution	Adj. SS	Adj. MS	F-Value	P Value
SiC (Wt.%)	2	269.198	81.70%	269.198	134.599	79.66	0.012
Tm (° C)	2	54.882	16.66%	54.882	27.441	16.24	0.058
S (rpm)	2	2.044	0.62%	2.044	1.022	0.6	0.623
Error	2	3.379	1.03%	3.379	1.69		
Total	8	329.504	100.00%				
S = 1.29987;		R-sq = 98.97%;		R-sq (adj) = 95.90%;			

Table 9 ANOVA analysis for tensile strength

Source	DF	Seq. SS	Contribution	Adj. SS	Adj. MS	F-Value	P Value
SiC (Wt.%)	2	0.000002	91.64%	0.000002	0.000001	717.22	0.001
Tm (° C)	2	0	7.48%	0	0	58.57	0.017
S (rpm)	2	0	0.75%	0	0	5.83	0.146
Error	2	0	0.13%	0			
Total	8	0.000002	100.00%				
S = 0.0000005;		R-sq = 99.87%;		R-sq (adj) = 99.49%;			

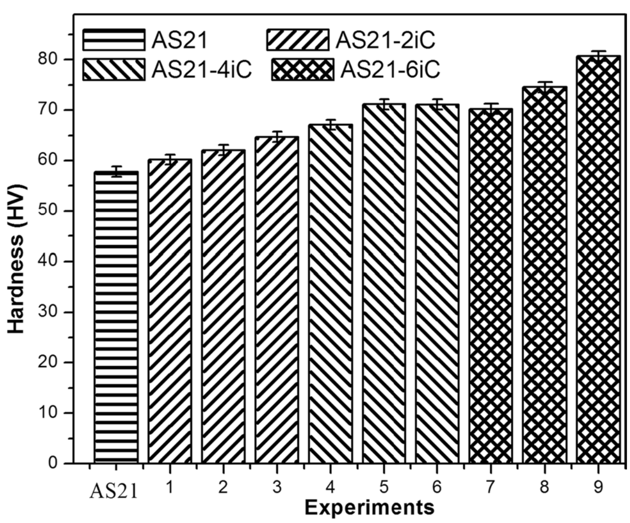

Fig. 8 Effect of SiC reinforcement for hardness of AS21 Mg composites

in as-cast AS21 Mg alloy (Fig. 2a) which exhibits the presence of large precipitate. The high silicon content (1.03%) in magnesium matrix may create high bonding force between elements leading to the clustering at the grain boundaries [33]. This observation is similar to structural changes of Mg-Si alloy through powder metallurgy developed by Seth [34].

To improve the microstructure of monolithic alloy, an SiC particulates were amalgamated into AS21 during two steps of stir-casting. Based on studies conducted by Palash [35], significant improvement in the microstructure and properties of Mg alloy through SiC addition. Cao [36] also summarized that the SiC particles were well bounded with Mg matrix by casting and shows no secondary phase between Mg/SiC interface. Addition of SiC reinforcement results in reduction in a size of the precipitate and refined microstructure of AS21 alloy (Fig. 5). The precipitate turned out to be finer with the weight fraction of SiC reinforcement during two-step stir-casting. This is due to SiC reinforcement restricts the grain growth and acts as heterogeneous nucleation sites of Mg grains [37].

The refined grains (Fig. 5) of AS21 alloy composite are due to reinforcement of SiC, leading to stimulation of nucleation in the primary phase. Anil Kumar [38] reported that the wettability of molten Mg and SiC directly influence the heterogeneous nucleation sites. The duel step stirring in the

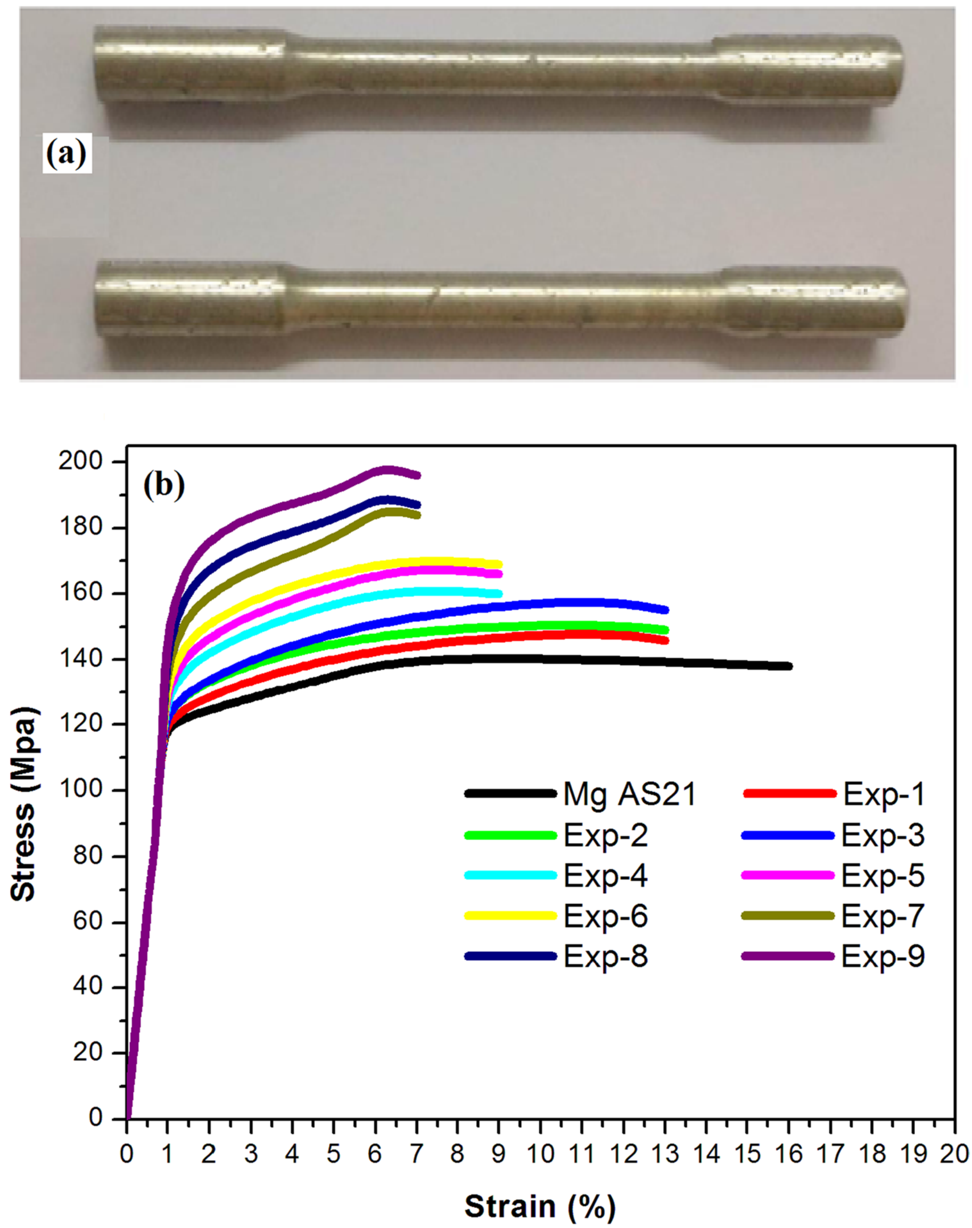

Fig. 9 Tensile test of AS21 Mg composites: (**a**) Test specimens; (**b**) Stress-strain curves

present work not only breaks the oxide layers and further to spread molten Mg on the surface of SiC particulates, leading to the improvement of wettability between Mg/SiC interface. This is the reason for refined grain structure as observed at high volume fraction (6 wt.%) of SiC reinforcement in AS21 matrix.

The hardness of SiC/AS21 composite (Fig. 8) is perpetually higher than the monolithic alloy. This is due to precipitation of fine Mg_2Si compound by SiC reinforcement, which aid to restriction of matrix deformation by constraining dislocation movement [18]. On the contrary, the appearance of coarse precipitates in AS21 alloy decreases the effectiveness in resisting the dislocation motion. This is the possible reason for registering less hardness values of AS21 alloy. The remarkable improvement with the addition of 6 wt.% of SiC reinforcement (Fig. 8) are due to the larger amount of the dislocations caused due to refine grain particles (Fig. 5d). Another possible reason is due to the creation of a large number of inhibition sites for dislocations movement by finer Mg_2Si phase [32].

With the addition of SiC reinforcement, the tensile strength of AS21 composites improved noticeably. SiC reinforcement not only prevents matrix deformation by limiting dislocation movement, but it also improves composite load bearing capacity [27]. Moreover, the precipitation of fine Mg_2Si compound caused by SiC reinforcement in a two-step process also contributed for strength enhancement of AS21 Mg composites. The tensile test in composites creates

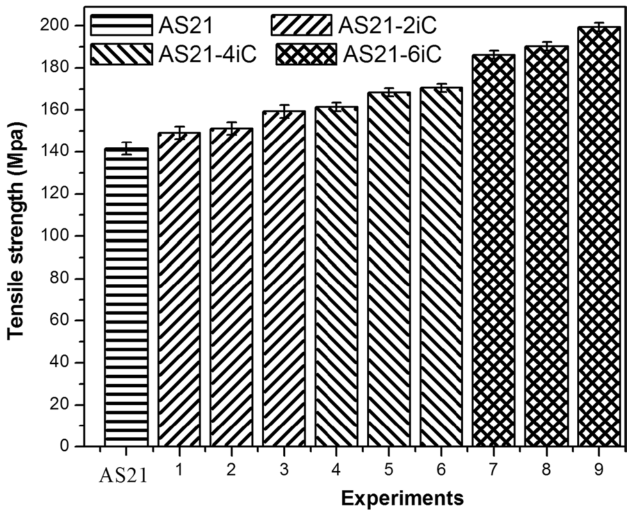

Fig. 10 Effect of SiC reinforcement for tensile strength of AS21 Mg composites

strong internal stress lead to crack formation at the interface between SiC and the intermetallic compound. But, when increasing the SiC concentration, the appearance of intermetallic compound in reinforcement region significantly reduced and size also finer [39]. This is the possible reason for strength enhancement of AS21 alloy by the addition of 2–6 wt.% of SiC reinforcement. Table 10 lists the mechanical properties of Mg alloy composites developed by others. The AS21 Mg alloy reinforced with 4% and 6% SiC fabricated through a two-step stir-casting attained comparable values.

4 Conclusions

Magnesium composite with AS21 ingot main matrix and reinforced with SiC reinforcement powders was successfully manufactured by dual step stir-casting route.

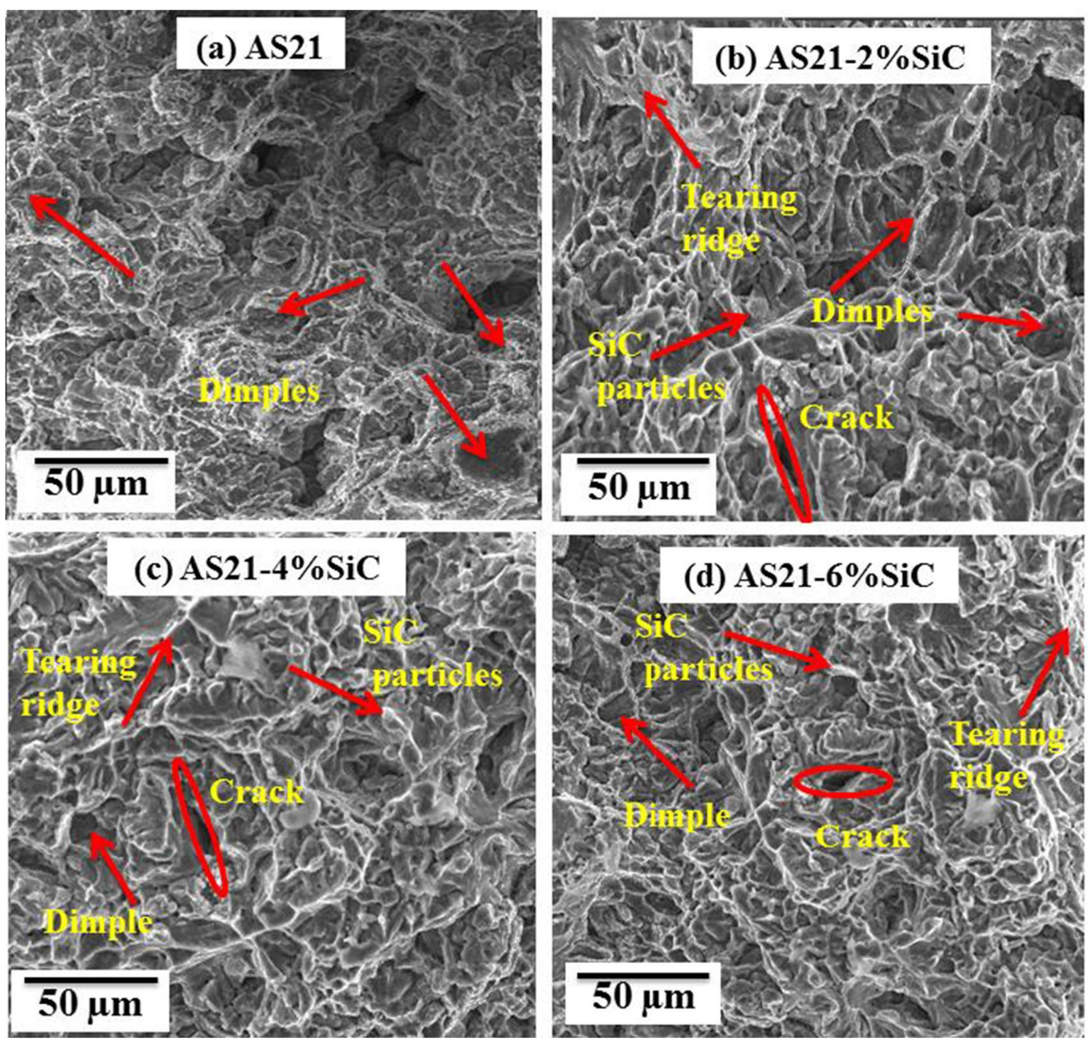

Fig. 11 Fracture surface morphology of AS21 composites: (**a**) 0% SiC; (**b**) 2% SiC; (**c**) 4% SiC; (**d**) 6% SiC

Table 10 Literature comparison with present work

Mg alloy	Reinforcement	Composition	Fabrication method	Hardness (HV)	Tensile strength (Mpa)	Reference
Mg	Nano-Y_2O_3	Mg + $2Y_2O_3$	Powder metallurgy	45	244	[40]
AZ91	Nano-SiC	AZ91 + SiC	Ultrasonic vibration	–	222	[41]
Mg	Nano-SiC	Mg + SiC	Stir-casting followed by Extrusion	39	224	[42]
AZ31B	Graphene	AZ31B + 0.3%Graphene	Stir-casting	93	196	[43]
AZ61	SiC	AZ61 + 2% SiC	Stir-casting	65	166.6	[44]
AZ91	SiC	AZ91 + 12% SiC	Vacuum assisted stir-casting	–	193.96	[38]
AZ91	SiC	AZ91 + 5% SiC	Stir-casting	82	181	[45]
AZ61	SiC	AZ91 + 1% SiC	Stir-casting	57.44	170	[46]
AS21	SiC	AZ91 + 4% SiC	Two-step Stir-casting	71.14 HV	170.51 MPa	Present work
AS21	SiC	AZ91 + 6% SiC		80.68 HV	199.35 MPa	

Microstructure and densification of SiC reinforcement elements on the AS21 matrix were investigated. Mechanical behaviour was analyzed by Taguchi optimization with three operating parameters and the conclusions derived from present work are given below.

1. Microstructural analysis Indicates that the AS21 alloy contains a coarse Mg_2Si precipitate that gets finer with SiC reinforcement. This precipitate was confirmed by SEM - EDS analysis. Furthermore, as the SiC reinforcement increased, the grain boundary refinement increased.
2. Density values of composite samples at various melt temperatures and stirring speeds were recorded. The highest value of 98.92% was determined in the composite fabricated at a melt temperature of 720 ^{o} C and stirring speed of 600 rpm.
3. The increase in SiC reinforcement and melt temperature lead to an increase in hardness of composites obtained. Addition of 2–6 wt.% of SiC contributed to the increase of AS21 alloy hardness by 10.67% and 28.35% respectively. The optimum condition to attain highest hardness in AS21/SiC composites could be estimated as 6 wt.% of SiC, melt temperature at 720 ^{o} C and stirring speed of 500 rpm.
4. The effect of SiC reinforcement on tensile strength of AZ21 alloy was revealed. Addition of 2–6 wt.% of SiC contributed to the increase of AS21 alloy strength by 11.06% and 28.92% respectively. The optimum condition to attain highest tensile strength in AS21/SiC composites could be estimated as 6 wt.% of SiC, melt temperature at 720 ^{o} C and stirring speed of 600 rpm.

Acknowledgments The authors acknowledge the Sophisticated Analytical Instruments Facility, DST-India for providing SEM facilities.

Author Contributions Conception and design of study: D Rognatha Rao

Acquisition of data: D Rognatha Rao

Analysis and/or interpretation of data: D Rognatha Rao

Drafting the manuscript: C Srinivas

Revising the manuscript critically for important intellectual content: D Rognatha Rao, C Srinivas

Funding The author(s) received no financial support for the research, authorship, and/or publication of this article.

Data Availability The authors confirm that the data supporting the findings of this study are available within the article and its supplementary materials.

Declaration

This article does not contain any studies with human or animal subjects.

Conflict of Interest The authors declare that there is no conflict of interest.

Consent to Participate Not applicable.

Consent for Publication Not applicable.

References

1. Basavarajappa S et al (2007) Application of Taguchi techniques to study dry sliding wear behaviour of metal matrix composites. Mater Des 28:1393–1398. https://doi.org/10.1016/j.matdes.2006.01.006
2. Davim P (2014) Metal matrix composites: materials, Manufacturing & Engineering, De Gruyter1st edition, edn, p ISBN: 978–3–11-031544-8
3. Jiangfeng S, Jia S et al (2020) Latest research advances on magnesium and magnesium alloys world wide. J Magnesium Alloys 8(1):1–41. https://doi.org/10.1016/j.jma.2020.02.003
4. Kumar CR et al (2020) Role of SiC on mechanical, Tribological and thermal expansion characteristics of B4C/talc-reinforced Al-6061 hybrid composite. Silicon 12:1491–1500. https://doi.org/10.1007/s12633-019-00243-0

5. Singh J, Jawalkar CS, Belokar RM (2020) Analysis of mechanical properties of AMC fabricated by vacuum stir casting process. Silicon 12:2433–2443. https://doi.org/10.1007/s12633-019-00338-8
6. Gruyter DE (2018) Wear of composite materials. 978–3–11-035298-6, Berlin, ISBN. https://doi.org/10.1515/9783110352986
7. Wong WLE, Gupta M (2006) Effect of hybrid length scales (micro + Nano) of SiC reinforcement on the properties of magnesium. Solid State Phenom 111:91–94
8. Prasanth S, Kaliamma K et al (2012) Microstructure and properties of stir cast AZ91 mg alloy-SiCp composites. Mater Sci Forum 710:365–370. https://doi.org/10.4028/www.scientific.net/MSF.710.365
9. Bhushan RK, Kumar S (2011) Influence of SiC particles distribution and their weight percentage on 7075 Al alloy. J Mater Eng Perform 20:317–323. https://doi.org/10.1007/s11665-010-9681-6
10. Huang S, Chen Z (2011) Grain refinement of AlNp/AZ91D magnesium metal-matrixcomposites. Kov Mater 49:259–264
11. Davim (Ed.). (2013), Tribology of nanocomposites. Springer Berlin Heidelberg. ISBN: 978–1–84821-352-4
12. Shen M, Wang X, Ying T, Wu K, Song W (2016) Characteristics and mechanical properties of magnesium matrix composites reinforced with micron/submicron/nanoSiC particles. J Alloy Compd 686:831–840
13. Hashim J, Looney L, Hashmi M (1999) Metal matrix composites: production by the stir casting method. J Mater Process Technol 92:1–7
14. Subbaiah V, Palampalle B, Brahmaraju K (2019) Microstructural analysis and mechanical properties of pure Al–GNPs composites by stir casting method. J InstEng India Ser C 100:493–500. https://doi.org/10.1007/s40032-018-0491-1
15. Tanwir A et al (2019) Optimization of wear behaviour using Taguchi and ANN of fabricated aluminium matrix nanocomposites by two-step stir casting. Mater Res Express 6:065002
16. Qiyao H, Haidong Z, Jilong G (2016) Microstructure and mechanical properties of (B4C+Al3Ti)/Al hybrid composites fabricated by a two-step stir casting process. Mater Sci Eng A 650:478–482. https://doi.org/10.1016/j.msea.2015.10.041
17. Pagidi M, Selvaraj N, Rao CSP, Veeresh K (2020) Fabrication and characterization two step stir casting with ultrasonic assisted novel AA7150-hBN nanocomposites. J Alloys Compd 815:152464. https://doi.org/10.1016/j.jallcom.2019.152464
18. Jiang QC, Wang HV, Wang Y, Ma BX, Wang JG (2005) Modification of Mg_2Si in mg–Si alloys with yttrium. Mater Sci Eng A 392:130–135. https://doi.org/10.1016/j.msea.2004.09.007
19. Luo AA (2004) Recent magnesium alloy development for elevated temperature applications. Int Mater Rev 49:13–30. https://doi.org/10.1179/095066004225010497
20. Hui-Yuan W, Wei W, Min Z et al (2008) Influence of the amount of KBF4 on the morphology of Mg_2Si in mg–5Si alloys. Mater Chem Phys 108:353–358. https://doi.org/10.1016/j.matchemphys.2007.10.006
21. Ye HZ, Liu XY (2004) Review of recent studies in magnesium matrix composites. J Mater Sci 39:6153–6171. https://doi.org/10.1023/B:JMSC.0000043583.47148.31
22. Kumar KC et al (2022) Microstructural, mechanical characterization, and Fractography of AZ31/SiC reinforced composites by stir casting method. Silicon 14:5017–5027. https://doi.org/10.1007/s12633-021-01180-7
23. Baradeswaran A, Elayaperumal A, Franklin I (2013) A statistical analysis of optimization of Wear behaviour of Al- Al_2O_3 composites using Taguchi technique. Procedia Eng 64:973–982. https://doi.org/10.1016/j.proeng.2013.09.174
24. Bellubbi S, Sathisha N, Mallick B (2022) Multi response optimization of ECDM process parameters for machining of microchannel in silica glass using Taguchi–GRA technique. Silicon 14:4249–4263. https://doi.org/10.1007/s12633-021-01167-4
25. Dey D, Biswas A (2021) Comparative study of physical, mechanical and Tribological properties of Al2024 alloy and SiC-TiB_2 composites. Silicon 13:1895–1906. https://doi.org/10.1007/s12633-020-00560-9
26. Bhowmik A, Dey D, Biswas A (2022) Characteristics study of physical, mechanical and Tribological behaviour of SiC/TiB2 dispersed Aluminium matrix composite. Silicon 14:1133–1146. https://doi.org/10.1007/s12633-020-00923-2
27. Matin A, Saniee FF, Abedi HR (2015) Microstructure and mechanical properties of mg/SiC and AZ80/SiC nanocomposites fabricated through stir casting method. Mater Sci Eng A 625:81–88. https://doi.org/10.1016/j.msea.2014.11.050
28. Rebillat F, Lamon J, Guette A (2000) The concept of a strong interface applied to SiC/SiC composites with a BN interphase. Acta Mater 48:4609–4618. https://doi.org/10.1016/S1359-6454(00)00247-0
29. Suhandani M, Puspitasari P, Abd R et al (2021) Impact, hardness and fracture morphology of Aluminium alloy (Al-Si) filled cobalt oxide nanoparticles at various stir casting temperatures. Malaysian J Composites Sci Manuf 5:11–20
30. Aravindan S, Rao PV, Ponappa K (2015) Evaluation of physical and mechanical properties of AZ91D/SiC composites by two step stir casting process. J Magnesium Alloys:52–62. https://doi.org/10.1016/j.jma.2014.12.008
31. Sambathkumar M et al (2017) Mechanical and corrosion behavior of Al7075 (hybrid) metal matrix composites by two step stir casting process. Latin Am J Solids Struct 14:243–255. https://doi.org/10.1590/1679-78253132
32. Guo EJ, Ma BX, Wang LP (2008) Modification of Mg2Si morphology in mg-Si alloys with bi. J Mater Process Technol 206:161e166. https://doi.org/10.1016/j.jmatprotec.2007.12.038
33. Liu YL, Kang SB, Kim HW (1999) The complex microstructures in an as-cast Al–mg–Si alloy. Mater Lett 41:267–272. https://doi.org/10.1016/S0167-577X(99)00141-X
34. Seth PP, Singh N (2020) Formation of fine Mg2Si phase in mg–Si alloy via solid-state sintering using high energy ball milling. J Alloys Compd 821:153205. https://doi.org/10.1016/j.jallcom.2019.153205
35. Poddar P, SrivastavaV C, De PK, Sahoo KL (2007) Processing and mechanical properties of SiC reinforced cast magnesium matrix composites by stir casting process. Mater Sci Eng A 460:357–364. https://doi.org/10.1016/j.msea.2007.01.052
36. Cao G, Choi H, Konishi H et al (2008) Mg–6Zn/1.5%SiC nanocomposites fabricated by ultrasonic cavitation-based solidification processing. J Mater Sci 43:5521–5526. https://doi.org/10.1007/s10853-008-2785-9
37. Gupta M, Nguyen QB, Hamouda AM, Tun KS, Minh NJ (2012) Investigation on the mechanical properties of mg-Al alloys (AZ41 and AZ51) and its composites. Metals (Basel) 2:313–328. https://doi.org/10.3390/met2030313
38. Kumar A et al (2018) Introduction to magnesium alloy processing technology and development of low-cost stir casting process for magnesium alloy and its composites. J Magnesium Alloys 6:245–254. https://doi.org/10.1016/j.jma.2018.05.006
39. Jayasathyakawin S, Ravichandran M (2022) Experimental investigations on effect of silicon carbide on microstructure and mechanical properties in mg-3 wt% Al alloy matrix using powder metallurgy. Silicon. https://doi.org/10.1007/s12633-022-01834-0
40. Khin ST, Gupta M (2007) Improving mechanical properties of magnesium using nano-yttria reinforcement and microwave assisted powder metallurgy method. Compos Sci Technol 67:2657–2664. https://doi.org/10.1016/j.compscitech.2007.03.006
41. Nie KB, Wang XJ, HuXS XL, Wu K, Zheng MY (2011) Microstructure and mechanical properties of SiC nanoparticles reinforced magnesium matrix composites fabricated by ultrasonic

vibration. Mater Sci Eng A 528:5278–5282. https://doi.org/10.1016/j.msea.2011.03.061

42. Choi H, Alba-Baena N, Nimityongskul S et al (2011) Characterization of hot extruded mg/SiC nanocomposites fabricated by casting. J Mater Sci 46:2991–2997. https://doi.org/10.1007/s10853-010-5176-y
43. Hao X, Guohong M, Jia Y, Yinshui H (2021) Preparation of graphene reinforced AZ31B magnesium-based composites by stirring casting, 110281. Vacuum 191. https://doi.org/10.1016/j.vacuum.2021.110281
44. Song-Jeng H, Addisu N (2019) Experimental investigations of effects of SiC contents and severe plastic deformation on the microstructure and mechanical properties of SiCp/AZ61 magnesium metal matrix composites. J Mater Process Technol 272:28–39. https://doi.org/10.1016/j.jmatprotec.2019.05.002
45. Saleh B, Jiang J, Fathi R et al (2020) Study of the microstructure and mechanical characteristics of AZ91–SiC_p composites fabricated by stir-casting. Archiv.Civ.Mech.Eng 20:71. https://doi.org/10.1007/s43452-020-00071-9
46. Huang SJ, Subramani M, Ali AN et al (2021) The effect of micro-SiCp content on the tensile and fatigue behavior of AZ61 magnesium alloy matrix composites. Inter Metalcast 15:780–793. https://doi.org/10.1007/s40962-020-00508-0